Safety Margin Ratio-Based Design of Isolation Gap Size for Base-isolated Structures

T. Nakazawa
Tokyo Kenchiku Structural Engineers, Co. Ltd., Japan

S. Kishiki
Osaka Institute of Technology, Japan

Z. Qu & A. Wada
Tokyo Institute of Technology, Japan

SUMMARY:
The risk of pounding against the surrounding structures, usually against the retaining walls, has become a major concern about the seismic performance of base-isolated buildings subjected to unexpectedly large earthquakes. The required isolation gap to ensure the superstructure of a base-isolated building not to collapse is evaluated through incremental dynamic analysis and the required gap size-to-seismic intensity relationship is established. From this relationship, two characteristic gap sizes, namely the minimum required gap size, δ_1, and the maximum gap size, δ_2, may be identified. Given a base-isolated building and a seismic intensity, e.g., the energy-equivalent velocity in this paper, an isolation gap wider than δ_1 would ensure a 50% possibility that the superstructure would not collapse. On the other hand, the isolation gap would impose no influence on the performance of the isolated building if it is wider than δ_2. Especially, the minimum required gap size, δ_1, is of essential importance for the performance design of base-isolated buildings. A simple equation of estimating δ_1 and δ_2 for buildings with various parameters is proposed through data regression. In addition, a procedure of determining the required strength for the superstructure, given a seismic intensity, is also proposed.

Keywords: base-isolated structure, isolation gap, incremental dynamic analysis, collision to retaining wall

1. INTRODUCTION

Compared with that of conventional seismic resistant building structures, the performance of a seismically isolated structure is relatively easier to estimate because of the well-controlled deformation pattern of the structure. However, it was pointed out that the performance of base-isolated structures might become suspicious and even unreliable under unexpectedly large earthquake (Kikuchi et al, 1995). In particular, possible poundings of the base of the superstructure against the retaining walls may subject the superstructure to unexpected damage. Recently, many efforts have been devoted in Japan to verifying the safety of base-isolated buildings under such extreme circumstances (for example, Sato et al, 2011; Ogura et al, 2011; Sano et al, 2010).

It has been widely accepted by structural engineers that the proportion of the isolation gap is of significant importance for ensuring the safety margin of a base-isolated building. However, the current common practice in Japan is to set the size of the isolation gap greater than the maximum displacement response of the isolation layer, obtained from dynamic analysis, to design-level earthquake ground motions. The uncertainty and variability of earthquake ground motions frequently urge the engineers to prefer isolation gap much wider than, sometimes even twice or thrice, the calculated maximum displacement to introduce some safety margin. Even though, the degree of safety margin is unclear. Furthermore, the construction site is usually limited and does not allow for too wide an isolation gap.

In this paper, the methodology of evaluating the seismic performance of building structures in FEMA P695 (2009) is adopted for base-isolated structures. Incremental dynamic analysis (IDA) is performed with a set of many ground motion records scaled incrementally until predefined ultimate limit state of the base-isolated building (Vamvatsikos and Cornell, 2002). The isolation gap size is thus related to a probabilistic limit state capacity of the building.

2. ANALYSIS MODEL

A two degree of freedom system as shown in Fig. 2.1 is adopted for the analysis. The superstructure is represented by a single degree of freedom with a nonlinear spring which exhibits a trilinear skeleton response and degraded reloading and unloading stiffness following the rules proposed by Takeda et al (1970) (Fig. 2.2(a)). As a standard case, the initial stiffness is assumed 6709×10^3 kN/m and the yield strength $Q_y = 45000$ kN. The total weight of the superstructure is assumed to be 150000 kN, resulting in 0.3 s fixed base period and a shear coefficient $C_0 = 0.3$. Furthermore, the cracking strength is assumed to be $0.3Q_y$, that is 13500 kN, in the standard case. The secant stiffness at the yield point is assumed to be 0.3 times the initial stiffness and the unloading stiffness parameter, β, defined by Takeda et al (1970) is taken as 0.4. 2% transient stiffness-proportional damping is assigned to the superstructure corresponding to its fixed-base period.
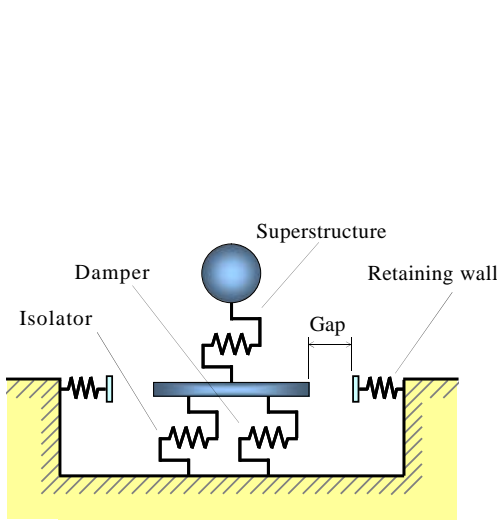
Figure 2.1. Analysis model
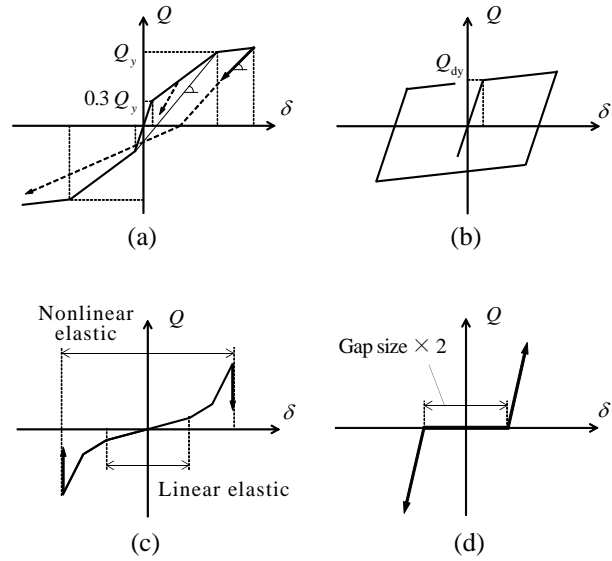
Figure 2.2. Hysteretic behavior: (a) superstructure; (b) damper; (c) isolation and (d) retaining wall

The weight of the isolation layer is assumed to be 40000 kN. The layer is modelled by three nonlinear springs in parallel, that is, a spring for dampers, a spring for isolators (rubber bearings) and a spring to simulate the pounding against the retaining walls. Bilinear elastic-plastic model is assumed for the damper spring (Fig. 2.2(b)). The yield strength of the dampers, Q_{dy}, is evaluated through the ratio of the yield strength of the dampers to the total weight of the whole building, denoted as α_s. It varies from 0.02 to 0.06 in the following analysis. The initial stiffness of the dampers is taken as 240×10^3 kN/m and the post-yield stiffness 4×10^3 kN/m.

It is assumed that natural rubber bearings are used as the isolators. Trilinear elastic hysteresis is adopted for the isolators (Fig. 2.2(c)). According to the test data in the literature, it is assumed that the isolator begins to exhibit strain-hardening at 250% shear strain and the tangent stiffness becomes 2 times the initial stiffness and then it further increases to 7 times the initial stiffness beyond 350% shear strain (Nakazawa et al, 2011). The bearing fractures at 450% shear strain. Two parameters of the isolator are investigated, namely the total rubber thickness, h, and the initial stiffness, k_i. Because the strain hardening and fracture of the isolator is defined by shear strain, the total rubber thickness has thus an influence on the deformation at which the isolator begins to harden and at which it fractures. On the other hand, the initial stiffness of the isolator, k_i, is generally used to calculate the so-called isolation period, T_f, which equals $2\pi\sqrt{(m/k_i)}$ and is an important characteristic vibration period for base-isolated buildings, where m is the total mass of the building, including the superstructure and the isolation layer. Although the total rubber thickness h has an influence on the stiffness of a single rubber bearing, it is a common practice in the design practice to use both sliding bearings and rubber bearings in a base-isolated building. As a result, the stiffness of the isolation layer can be adjusted by changing the proportion between the sliding and the rubber bearings without changing the rubber thickness of

the rubber bearings. Hence, the two parameters, h and k_i, are able to be considered independent of each other.

The post-fracture behavior of the bearing is not modelled. Instead, a very large stiffness is assigned to the bearing when it exceeds the fracture strain. In real cases, the superstructure may fall down on the lower footings and the friction on the contact interface, whose friction coefficient is believed greater than 0.4, is large enough to prevent any further displacement of the isolation layer before the superstructure collapses.

Pounding is modelled by a linear spring with initial gaps on both sides of the origin (Fig. 2.2(d)). The stiffness of the retaining wall is set to be 575×10^3 kN/m as a standard. This value is derived by assuming a 50 m long cantilever retaining wall, whose unit meter stiffness is based on the stiffness of a 7 m high reinforced concrete cantilever wall with soil backfill suggested by Kashiwa et al (2005). Influenced by the properties of the backfill soil and the thickness of concrete wall, the stiffness of the retaining wall is subject to great uncertainty. To address this uncertainty, the retaining wall stiffness is taken as 1/100, 1/50, 1/10, 1/5, 1.0 and 2.0 times the standard stiffness, that is, 575×10^3 kN/m, in the following analysis to see its effect. These ratios are denoted as β_k hereafter.

3. INPUT GROUND MOTIONS

The Far-Field set in FEMA P695 (2009) is used as the input ground motions in the following analysis. Among the 44 earthquake ground motion components in the Far-Field set, however, there are 8 components, belonging to 6 different records, whose maximum usable period are less than 6 s. Because the isolation period of 6 s will be investigated, these components are considered inappropriate. So the 6 records containing these unqualified components are excluded in the analysis and the remaining 32 components of 16 records are used. The two components in a record are used independently in the analysis. In addition, they are also normalized independently by their respective peak ground velocity (PGV) to the median PGV of the 32 components.

After being normalized, the ground motion set is ready for the use in the incremental dynamic analysis (IDA), in which the ground motions are scaled selectively to produce different earthquake intensities. In FEMA P695 (2009), the spectral acceleration corresponding to the fundamental period of vibration, $S_a(T_1)$, is used as the intensity measure. For base-isolated structures, some equivalent period is usually a better indicator for the dynamic response of the building than the fundamental period. In practical design, such equivalent period is generally related to the secant stiffness of the isolation layer at its maximum deformation response. In IDA, however, the maximum deformation of the isolation layer changes constantly with the change in earthquake intensity. It is not easy to define a uniform equivalent stiffness for a single isolated building subjected to ground motions of various intensities. As a result, the above mentioned isolation period T_f, which is independent of the structural response, is considered a better quantity to represent the dynamic characteristic property of the building.

On the other hand, it has become a common practice to use the energy-equivalent spectral velocity, V_E, as intensity measure for flexible structural system (in Japan) (Akiyama, 1980). V_E is the velocity which makes the kinematic energy of the total mass of a system equals its input energy of the system under the ground motion. As a result, the energy-equivalent spectral velocity corresponding to the isolation period, $V_E(T_f)$, is used as the intensity measure in this study. Fig. 3.1 gives an example when the 32 ground motions, after being normalized by their PGVs, are selectively scaled to a median $V_E(T_f)$ = 150 cm/s at T_f = 4 s.
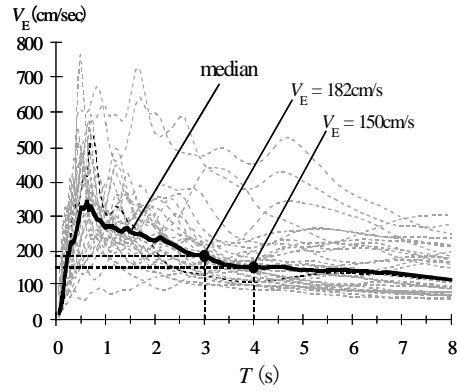
Figure 3.1. Scaling of ground motions

4. EVALUATION OF ISOLATION GAP SIZE

4.1. Evaluation method

The IDA curves of an isolated building with $C_0 = 0.25$, $T_f = 4$ s, $h = 200$mm, $\alpha_s = 0.04$, $\beta_k = 1$ and gap size = 50 cm are illustrated in the left graph in Fig. 4.1(a). The bold line indicates the median of the individual curves. It is seen that almost all the IDA curves tend to enter a flat branch before the superstructure yields (i.e., its ductility factor, μ, which is the ratio of the maximum to the yield displacement, exceeds 1.0). This indicates the great effect of pounding. This is otherwise for an isolated building with gap size = 70 cm and all other parameters the same, as can be seen in Fig. 4.1(b).
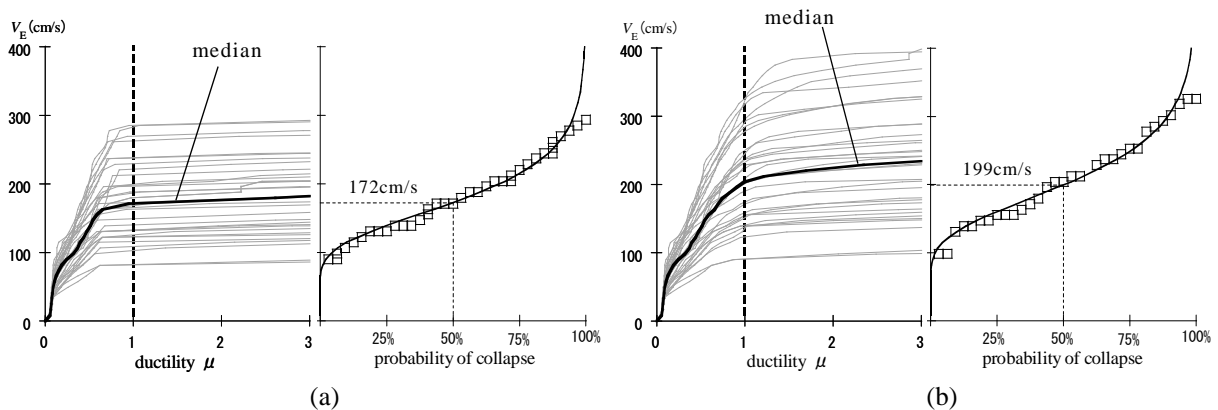
Figure 4.1. Evaluation of collapse capacity: (a) gap size = 50 cm and (b) gap size = 70 cm

In common practice, the superstructure of an isolated building is not subject to strict requirement for ductile behavior. Therefore, it seems realistic to define the collapse of the superstructure when its ductility μ exceeds 1.0. The intensity measure, V_E, corresponding to $\mu = 1.0$ for every ground motion can be collected and a collapse fragility curve can thus be produced, as demonstrated in the right graphs in Fig. 4.1(a) and (b), which relates the intensity measure, V_E, with the probability of collapse. The V_E corresponding to 50% probability of collapse is then determined by fitting the data to a lognormal distribution function. The thus-obtained V_E is defined herein as the collapse capacity, denoted as V_{EC} hereafter.

4.2. Characteristic gap sizes

A change of any of the structural parameters described above will have more or less an influence on V_{EC} of a base-isolated building. Particularly, the influence of the gap size is of great interest of the

present paper. Fig. 4.2 shows the relationship of V_{EC} and gap size for isolated building with $T_f = 4$ s., $h = 200$mm, $\alpha_s = 0.04$, $\beta_k = 1$. For all the value of C_0, essentially bilinear relationship can be observed It can also be observed that larger C_0 increases the gap size at which the curve enters a flat branch.

Given a design requirement of collapse capacity, for example, $V_{EC} = 150$ cm/s as shown in Fig. 4.2, a corresponding gap size can be found from the V_{EC}-gap size curve. This gap size is the minimum size necessary to ensure the required collapse capacity, and is denoted as δ_1 hereafter. On the other hand, the gap size would have nothing to do with the collapse capacity when it exceeds a certain value, that is, the V_{EC}-gap size curve becomes flat. This certain value, as marked in Fig. 4.2 as hollow circles, is denoted as δ_2. It indicates a maximum gap size until which the gap size has an effect on the performance of the building. It is highly dependent on the strength of the superstructure, C_0.

In addition, there are cases that the building cannot meet the collapse capacity requirement even if the gap size is infinite or the pounding is not taken into account. For example, it is so when $C_0 = 0.15$ as shown in Fig. 4.2(b). In this case, the design of the base-isolated building itself, rather than the selection of an appropriate gap size, should be revised.
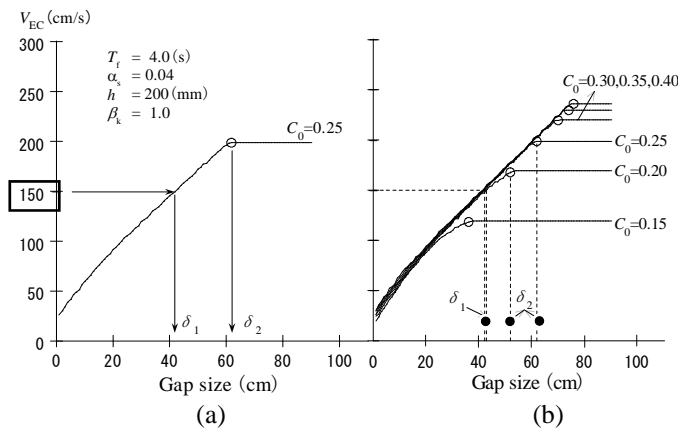
Figure 4.2. Definition of characteristic gap sizes δ_1 and δ_2: (a) $C_0 = 0.25$ and (b) $C_0 = 0.15 \sim 0.40$

4.3. Influence of structural properties

Other structural properties may have influence on the relationship of collapse capacity versus gap size. In Fig. 4.3(a), the relationships for building of isolation period $T_f = 3$ s and $T_f = 6$ s are compared. Longer isolation periods indicate softer isolators used in the isolation layer. This generally leads to two major consequences, that is, on one hand, less strength demand for the superstructure; and on the other hand, greater displacement response of the isolation layer, given input energy the same. As a result, as can be seen in Fig. 4.3(a), provided the gap is infinite, the collapse capacities of $T_f = 6$ s buildings are greater than those of $T_f = 3$ s ones, given the strength of the superstructure the same. On the other hand, however, the required minimum gap sizes, δ_1, for $T_f = 6$ s buildings are much larger than those for buildings of $T_f = 3$ s, given the demand for collapse capacity the same.

Another structural property having major influence on δ_1 is the amount of dampers in the isolation layer, which is represented by the ratio α_s. It seems that the increase of the amount of dampers can help reducing δ_1 given the demand for collapse capacity the same. This is demonstrated in Fig. 4.3(b) by comparing the results for buildings of $\alpha_s = 0.02$ and for those of $\alpha_s = 0.06$. However, it is worth noting that the increase in the amount of dampers also increase the strength demand for the superstructure.

The total height of the rubber, h, also has an effect on the V_{EC}-gap size curves, but this effect seems to confine to only δ_2, the maximum effectual gap size(Fig. 4.3(c)). Smaller rubber height means that the isolator would exhibit strain hardening and thus subject the superstructure to large shear force at smaller deformation. This is another effective restrain for an isolated building to develop greater collapse capacity, other than the restrain from the isolation gap size.

Finally, the stiffness of the retaining wall has some effect on the performance of the isolated building. However, this is true only if the retaining wall stiffness is comparable or even smaller than the stiffness of the isolator. To give an example, the V_{EC}-gap size curves for buildings with very soft retaining walls ($\beta_k = 1/100$) are compared with those for buildings with very stiff walls ($\beta_k = 2$). In this example, the retaining wall stiffness in the former case is only 0.12 times while that in the latter case is 24 times the isolator stiffness. Significant difference between the two cases can be observed(Fig. 4.3(d)). Very soft a retaining wall practically reduces the required gap size to attain a certain collapse capacity. It even sometimes completely diminishes the necessity of setting any criterion for the gap size because the retaining walls are so soft that they could rarely have significant effect on the performance of the building. On the other hand, however, the difference between stiff walls and even stiffer walls is almost negligible. For example, the results with $\beta_k = 1.0$ (see Fig.4.3(c) for reference, although the rubber thickness is different) and those with $\beta_k = 2.0$ are almost identical.
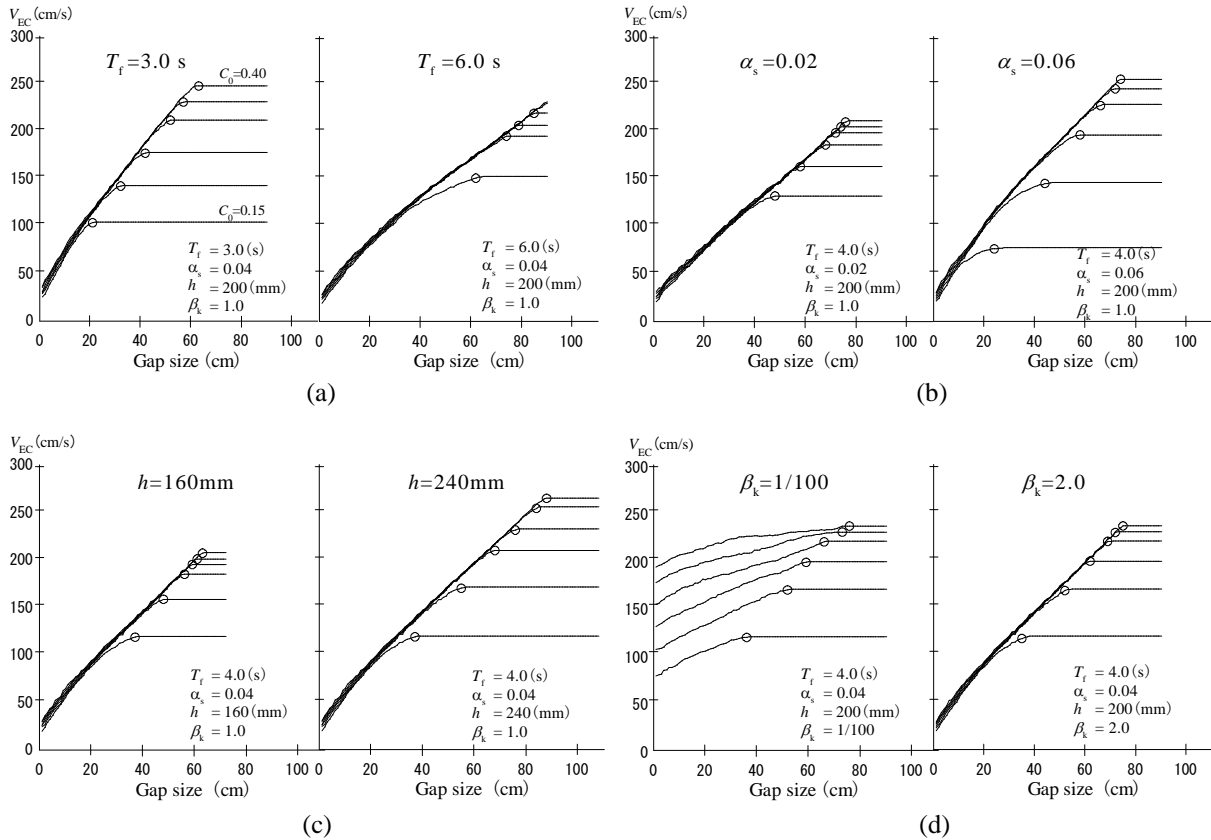
Figure 4.3. Influence of structural properties: (a) isolation period; (b) amount of dampers; (c) total height of rubber and (d) stiffness of retaining wall

5. SIMPLIFIED EQUATIONS

Because it is not convenient to demonstrate all the effects of various structural parameters on the collapse capacity and the required gap size through the above V_{EC}-gap size curves, especially when these effects become interdependent, some simplified equations describing the relationship between V_{EC} and characteristic gap sizes, δ_1 and δ_2, and the influence of some primary parameters would be useful for engineers in their practical design.

In order to simplify the calculation of the minimum required gap size, δ_1, the ascending branch of the V_{EC}-gap size curve obtained in the above described analysis is linearized. The parts corresponding to very small and very large collapse capacities are removed from the linearization. Practically, a straight

line is produced by simply connecting the data point closest to $V_{EC} = 80$ cm/s and the one closest to $V_{EC} = 240$ cm/s, as shown in Fig. 5.1(b). For cases where the maximum V_{EC} (that is the one corresponding to $C_0 = 0.4$) is less than 240 cm/s, the point at the maximum V_{EC} is used (see Fig. 5.1(a)).
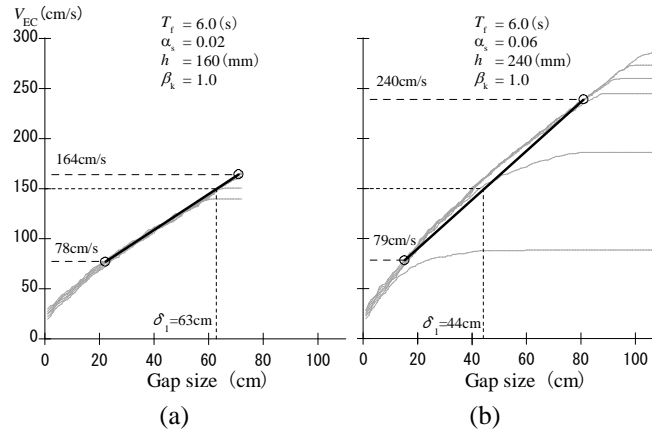
Figure 5.1. Linearization for calculating δ_1: (a) $\alpha_s = 0.02$, $h = 160$ mm and (b) $\alpha_s = 0.06$, $h = 240$ mm

For δ_2, the linearization is a little more complicated. First, two points are identified on a single V_{EC}-gap size curve, that is, the point at which the gap size finally has no more influence on V_{EC}, for example, those marked as hollow circles 'o' in Fig. 5.2., and the point at which the curve begin to deviate from that of a greater C_0, for example, those marked as '×' in Fig. 5.2. Then the point shares the same V_{EC} with the '×' point and the same gap size with the 'o' point is found, like those marked as hollow triangles 'Δ' in Fig. 5.2. Finally, these triangle points are regressed to a straight line by least-squares fitting. Given a demand for collapse capacity, the corresponding δ_2 can be read from this straight line. With this δ_2, a strength demand for the superstructure can then be obtained on the restoring force skeleton curve of the isolation layer, as is shown in Fig. 5.2.
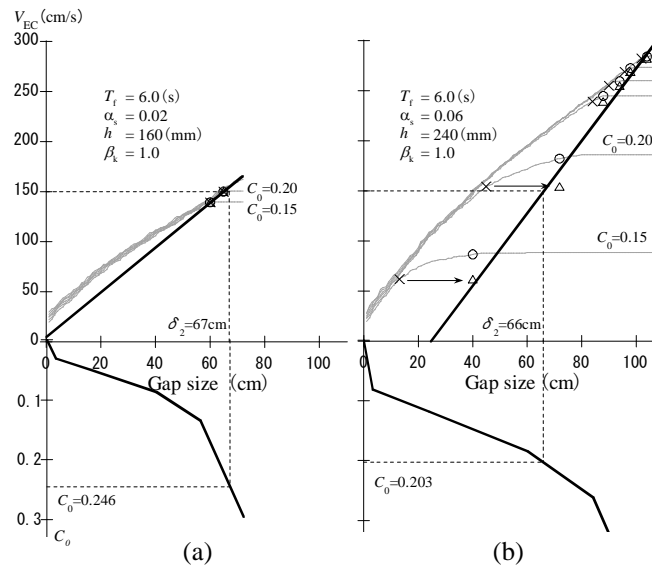
Figure 5.2. Linearization for calculating δ_2: (a) $\alpha_s = 0.02$, $h = 160$ mm and (b) $\alpha_s = 0.06$, $h = 240$ mm

Through data fitting, two extreme points on each of the above straight lines, that is, one at δ_1 or $\delta_2 = 0$ cm and the other at δ_1 or $\delta_2 = 108$ cm, are expressed as functions of two primary influencing parameters, the isolation period, T_f, and the amount of dampers, α_s. The function has the form as shown in Eqn. 5.1. It should be noted that this equation is obtain by data fitting and the data range is between $V_{EC} = 80$ cm/s and $V_{EC} = 240$ cm/s. In addition, δ_2 should always be smaller than the fracture deformation of the isolator. The degree of approximation is demonstrated in Fig. 5.3 for the two extreme points. It

suggests that the proposed equation generally captures the trend of variation of the collapse capacity, V_{EC}. Given a demand for collapse capacity, the corresponding δ_1 and δ_2 can be obtained by interpolating between the two extreme points, that is, V_{EC} at δ_1 or $\delta_2 = 0$ cm and V_{EC} at δ_1 or $\delta_2 = 108$ cm.

$$V_{EC} = a \cdot T_f^2 + b \cdot T_f + c \qquad (5.1)$$

where the value of coefficient a, b and c is given in Table 5.1.

Table 5.1. Coefficients in Eqn. 5.1

	a	b	c
$\delta_1=0$cm	0	0	34
$\delta_1=108$cm	$150\alpha_s+10.6$	$-1440\alpha_s-140$	$5340\alpha_s+630$
$\delta_2=0$cm	0	$440\alpha_s-44$	$-1070\alpha_s+135$
$\delta_2=108$cm	$150\alpha_s+10.6$	$-1440\alpha_s-140$	$5340\alpha_s+630$
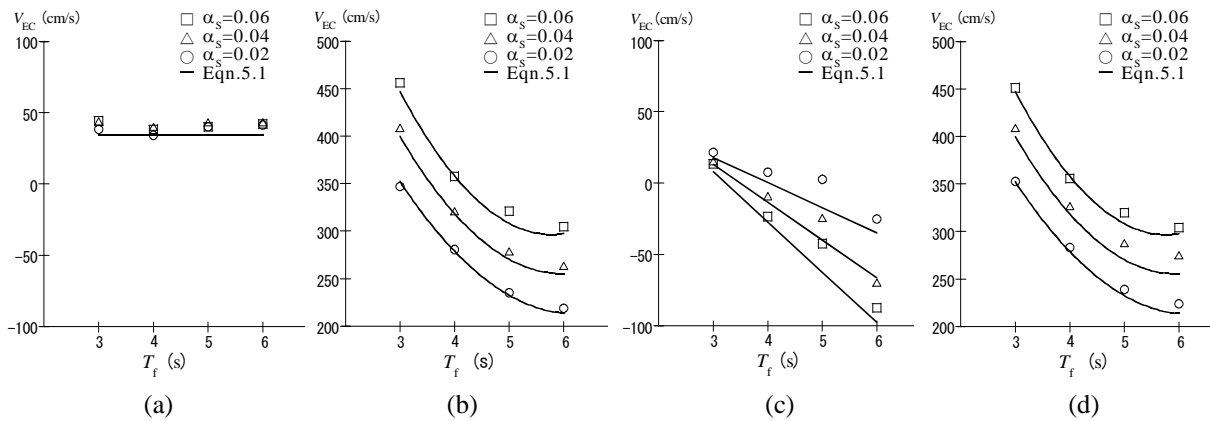
Figure 5.3. Results from analysis and simplified equation: (a) $\delta_1 = 0$ cm; (b) $\delta_1 = 108$ cm; (c) $\delta_2 = 0$ cm and (d) $\delta_2 = 108$ cm

6. CONCLUSIONS

The following conclusions may be drawn from the above discussions.

(1) Collapse capacity is defined for seismically isolated buildings in terms of energy-equivalent spectral velocity through incremental dynamic analysis. This capacity is found to have an essentially bilinear relationship with the isolation gap size of the building.

(2) Given the demand for the collapse capacity of an isolated building, the minimum required gap size to attain this demand, denoted as δ_1, can be found.

(3) Another characteristic gap size, beyond which the gap size would have no more influence on the collapse capacity of the building structure, denoted as δ_2, is also recognized. It is practically the turning point of the above mentioned bilinear relationship. Through δ_2, the necessary strength of the superstructure to attain the required collapse capacity can be determined.

(4) Any gap size greater than δ_1 should be acceptable in practical design. With the capacity versus gap size relationship, the benefit of using gap size greater than δ_1 can be quantified in terms of the increase in the collapse capacity of the building.

(5) A simplified equation of calculating δ_1 and δ_2 for any given demand of collapse capacity is established by data fitting. It may serve as a convenient tool for engineers in proportioning the isolation gap size.

REFERENCES

Akiyama H. (1980). *Earthquake-resistant limit-state design for buildings*. The University of Tokyo.

FEMA P695 (2009). *Quantification of building seismic performance factors*. Federal Emergency Management Agency, Washington, D.C.

Kashiwa H, Nakayasu N and Nakashima M. (2005). Response and damage of base-isolated buildings subjected to very large earthquakes. *Journal of Structural Engineering, AIJ*, **51B**: 237-246.

Kikuchi M, Tamura K and Wada A. (1995). Safety evaluation of base-isolated structures. *Journal of Structural Construction and Engineering, AIJ*, 470: 65-73.

Nakazawa T, Kishiki S, Qu Z, Miyoshi A and Wada A. (2011). Fundamental study on probabilistic evaluation of the ultimate state of base isolated structures. *Journal of Structural and Construction Engineering, AIJ*, **76**(662): 745-754

Ogura M, Maeno T, Kondo K, Fujitani H, Hayashi Y and Kuramoto H.(2011).Research on Design Earthquake Ground Motion and Design Method of Building for Uemachi Fault Earthquake Part8 : Design Method of Base-Isolated Structure, Summaries of technical papers of AIJ annual meeting, **B-2**: 551-552.

Sano T, Miwada G, Katsumata H, Komaki J, Sato K, Takiyama N and Hayashi Y. (2010). Experiments of collision to retaining wall with real scale base-isolated building: Part 1~5, *Summaries of technical papers of AIJ annual meeting*, **B-2**: 427-436.

Sato K, Komaki J, Miwada G, Sano T, Katsumata H, Takiyama N and Hayashi Y. (2011). Seismic Response Prediction for Base-isolated Buildings in Collision to Retaining Wall Including the Soil Behind, Summaries of technical papers of AIJ annual meeting, **B-2**: 483-484.

Takeda T, Sozen MA and Nielsen NN. (1970). Reinforced concrete response to Simulated Earthquakes. *Journal Structural Division, ASCE*, **96**(ST12),2257-2573.

Vamvatsikos D and Cornell CA. (2002). Incremental dynamic analysis. *Earthquake Engineering and Structural Dynamics*, **31**(3), 491- 514.